

Synthesis, structure and dioxygen reactivity of Ni(II) complexes with mono-, bis-, tetra- and hexa-oxime ligands



Yaroslav D. Boyko^a, Alexey Yu. Sukhorukov^{b,*}, Artem N. Semakin^b, Yulia V. Nelyubina^c, Ivan V. Ananyev^c, K.S. Rangappa^d, Sema L. Ioffe^b

^a Higher Chemical College RAS, Miuskaya square 9, 125047 Moscow, Russia

^b N.D. Zelinsky Institute of Organic Chemistry, Leninsky prospect 47, 119991 Moscow, Russia

^c A.N. Nesmeyanov Institute of Organoelement Compounds, Vavilov str. 28, 119991 Moscow, Russia

^d University of Mysore, Crawford Hall, Mysore 570 005, Karnataka, India

ARTICLE INFO

Article history:

Received 29 October 2013

Accepted 1 January 2014

Available online 10 January 2014

Keywords:

β-(Oximinoalkyl)amines

Ni(II) chelates

Oxime complexes

Aerobic oxidation

ABSTRACT

Four nickel complexes with β-(oximinoalkyl)amine ligands Ox_nH_n containing one (Ox₁H₁), two (Ox₂H₂), four (Ox₄H₄) and six (Ox₆H₆) oxime groups were synthesized and characterized by elemental analysis, FTIR, HRMS and single crystal X-ray diffraction. β-Oximinoalkylamines Ox_nH_n act as polydentate ligands forming five-membered chelate rings, in which nickel is coordinated with both amine and oxime nitrogen atoms. In all structurally characterized complexes, OH-groups of oxime arms are involved in hydrogen bonding with counterions (Cl⁻), which are located in the inner or outer coordination sphere of the nickel atom. Two new structural types of pseudo-octahedral Ni(II) β-oximinoalkylamine complexes containing two ligands per one nickel ion (Ni(Ox₁H₁)₂Cl₂ and Ni(Ox₂H₂)₂Cl₂) were identified. Dioxygen reactivity of the obtained complexes in aerobic oxidation of triphenylphosphine was studied. Bis-oxime complex Ni(Ox₂H₂)₂Cl₂ was found to be the most active promoter of triphenylphosphine oxidation among the synthesized nickel complexes.

© 2014 Elsevier Ltd. All rights reserved.

1. Introduction

Oxidation is one of the most important chemical transformations employed in the synthesis of many versatile organic compounds [1]. Industrial oxidation processes usually produce many waste products and require harsh conditions (high temperature, pressure) as well as application of expensive catalysts and highly reactive non-selective oxidative agents [1]. In nature, however, oxidative transformations proceed smoothly and efficiently at ambient temperature with molecular oxygen as oxidant under catalysis by oxidase and oxygenase enzymes [2]. Among these processes are well-known oxidation of lipids and steroids with dioxygen catalyzed by cytochrome P450 family metalloenzymes [2c], aerobic oxidation of CH₄ to methanol by methanotrophic bacteria catalyzed by methanemonooxygenase enzyme [2d] and some others [2]. From the industrial standpoint, molecular oxygen is the most available, economically beneficial and ecologically-friendly oxidant [3]. In modern organic chemistry, however, not much examples of selective aerobic oxidation at ambient temperature are known [4] due to the absence of efficient catalysts, which mimic natural metalloenzymes. In this context, design and study of

new catalytic systems for biomimetic oxidation reactions is important for the development of innovative green processes as well as understanding of the mechanism of oxidases and oxygenases action [5].

In the recent years, a number of oxidative transformations of organic substrates by molecular oxygen employing catalytic systems based on copper [2e,4b], iron [4c], manganese [4d] and some other metal complexes [4,5] were discovered. In this regard, nickel complexes are much poorly explored [4d], probably, because of high potential of Ni(II) oxidation to higher oxidation states (i.e. Ni(III) and Ni(IV)) [6]. Only in 2004 Baldwin and coauthors reported the first nickel-promoted aerobic oxidation of simple organic compounds (methanol, benzylamine, triphenylphosphine) without the oxidative destruction of ligand [7]. The reaction was promoted by a deprotonated Ni(II) complex with a tripodal ligand tris(β-oximinoalkyl)amine Ox₃H₃ (Ni(Ox₃H₃)(NO₃)₂(H₂O)₂, Fig. 1) [6,7]. A distinctive feature of Ox₃H₃ is its ability to stabilize higher oxidation states of nickel with three anionic oximate groups generated upon deprotonation of oxime fragments (for stabilization of nickel in higher oxidation state by oximate groups see Refs. [6,8]). Dinuclear oximate-bridged nickel complexes generated upon deprotonation of Ni(Ox₃H₃)(NO₃)₂ reversibly react with molecular oxygen at ambient temperature forming Ni(III) iminoxyl radical complexes, which then oxidize the organic substrate [7].

* Corresponding author. Tel.: +7 4991355329; fax: +7 4991355328.

E-mail address: sukhorukov@ioc.ac.ru (A.Yu. Sukhorukov).

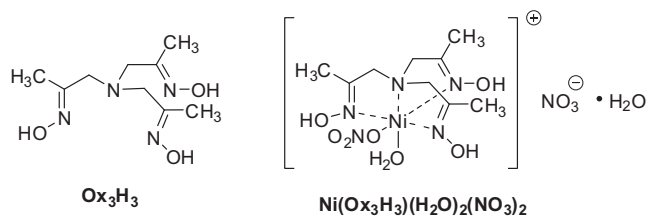


Fig. 1. Tris-oxime Ox_3H_3 and its Ni(II) complex.

To date, however, it is not known whether other nickel complexes of (β -oximinoalkyl)amine ligands are able to promote aerobic oxidation and what are minimal ligand structure requirements for realization of this process. In particular, it is interesting how the number of oxime groups in the ligand affects the dioxygen reactivity of corresponding nickel complexes. In the present work, a series of previously unknown analogues of nickel Ox_3H_3 complexes containing ligands with one (Ox_1H_1), two (Ox_2H_2), four (Ox_4H_4) and six (Ox_6H_6) oxime groups (Fig. 2) were obtained, structurally characterized and studied in the aerobic oxidation of triphenylphosphine as model substrate.

2. Experimental

2.1. General remarks

All reactions were performed in oven-dried (150 °C) glassware. Catalytic hydrogenations were carried out in a steel autoclave with external stirring and heating. Column chromatography was performed using Silica gel 40–60 μm 60A (Acros Organics). CH_2Cl_2 (technical grade), MeCN (technical grade), Et_3N , Me_3SiCl and Me_3SiN_3 were redistilled from CaH_2 , acetone was redistilled from Na_2SO_4 . Hexane, EtOAc and methanol were distilled without drying agents. $\text{NiCl}_2 \cdot 6\text{H}_2\text{O}$, $\text{Ni}(\text{NO}_3)_2 \cdot 6\text{H}_2\text{O}$, $\text{Ni}(\text{ClO}_4)_2 \cdot 6\text{H}_2\text{O}$, ethylenediamine, tris(aminoethyl)amine (tren), 5%–Pd/C were purchased from commercial sources and used as received.

HRMS were measured on electrospray ionization (ESI) instrument with a time-of-flight (TOF) detector. FTIR spectra were recorded on Bruker Vector22 and Bruker Alpha spectrometers in KBr pellets. UV–Vis spectra were recorded on Shimadzu UVmini-1240 and Shimadzu UV-2600 spectrometer. Peaks in IR and UV–Vis spectra data are reported with the following relative intensities: s (strong), m (medium), w (weak), br (broad), sh (shoulder).

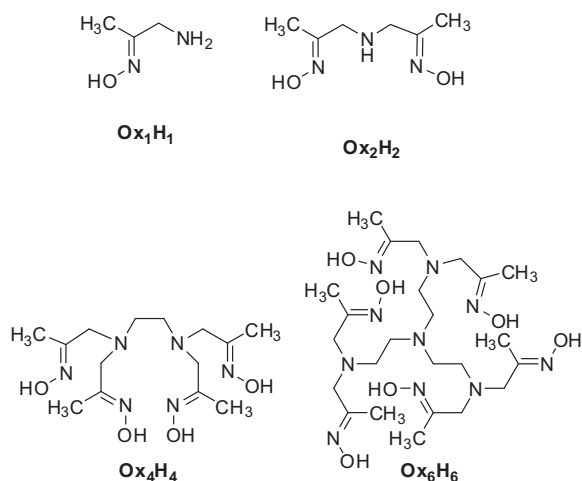


Fig. 2. Ox_nH_n ligands ($n = 1, 2, 4$ and 6).

Elemental analysis was performed by the Analytical Laboratory of the Institute of Organic Chemistry. NMR spectra were recorded at room temperature on a Bruker AM 300 spectrometer. The chemical shifts (^1H , ^{13}C) are given ppm (δ) in relative to the solvent signal. Multiplicities are indicated by s (singlet), d (doublet), t (triplet), q (quartet), m (multiplet), br (broad). Analytical thin-layer chromatography was performed on silica gel plates with QF-254. Visualization was accomplished with UV light or the solution of ninhydrin/ H_2SO_4 in ethanol.

2.2. Preparation of ligands and complexes

Complexes $\text{Ni}(\text{Ox}_3\text{H}_3)(\text{NO}_3)_2(\text{H}_2\text{O})_2$ [6] and $\text{Ni}(\text{Ox}_3\text{H}_3)\text{Cl}_2$ [11,13] were prepared according to previously described procedures. Ligands Ox_3H_3 [9a] and Ox_1H_1 [9b] were prepared according to literature methods from 2-nitropropane *via* intermediacy of bis(siloxy)enamine **1** [10] and α -azidooxime **2** (Scheme 1, see discussion in Section 3.1) [12].

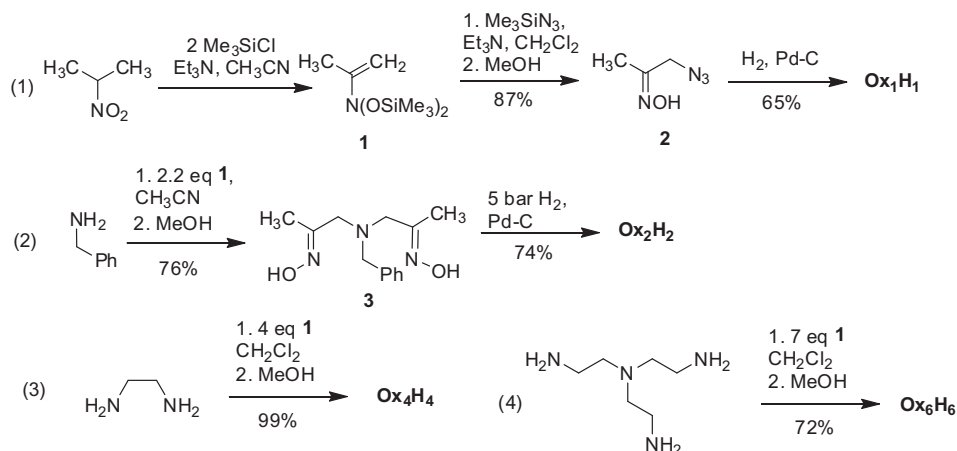
2.2.1. General procedure for the preparation of oximes **3**, Ox_4H_4 and Ox_6H_6

To a stirred solution of 1 mmol of an appropriate amine (benzylamine for **3**, ethylenediamine for Ox_4H_4 , tris(aminoethyl)amine for Ox_6H_6) in CH_2Cl_2 (2 mL) was added 1 M solution of bis(siloxy)enamine **1** (2.2 mL for **3**, 4 mL for Ox_4H_4 , 7 mL for Ox_6H_6) in CH_2Cl_2 . The reaction solution was kept at r.t. for 24 h and then quenched with MeOH (30 mL). After 30 min the solution was concentrated in vacuum. The residue was preadsorbed on silica gel and subjected to a column chromatography on silica gel (eluent: ethyl acetate/hexane = 1:3 \rightarrow 1:1 \rightarrow ethyl acetate for **3**, ethyl acetate \rightarrow ethyl acetate/MeOH = 10:1 \rightarrow 5:1 \rightarrow 1:1 for Ox_6H_6). Oxime Ox_4H_4 was isolated by crystallization from ethyl acetate/MeOH mixture. Yields: 76% (**3**), 99% (Ox_4H_4), 72% (Ox_6H_6). ^1H NMR spectra of oximes **3** [9b] and Ox_4H_4 [9a] are consistent with literature data. FTIR (Ox_4H_4), cm^{-1} : 3197s,br; 3105s,br; 2957s; 2879s,sh; 2823s; 2723m; 1667m; 1464s,sh; 1443s,sh; 1370s,sh; 1266s,sh; 1246s; 1141m; 1106m; 1054s; 1040s; 1021s; 972s; 938s; 869m; 837m; 807m,br; 675s; 548w; 478w.

1-((2-(bis(2-(bis(*E*)-2-(hydroxyimino)propyl)amino)ethyl)amino)ethyl)((*E*)-2-(hydroxyimino)propyl)amino)propan-2-one oxime (Ox_6H_6). White foam. ^1H NMR (300 MHz, $\text{DMSO}-d_6$): $\delta = 1.74$ (s, 18 H, 6 CH_3), 2.3–2.6 (m, 12 H, $-\text{CH}_2-\text{CH}_2-\text{N}$), 2.95 (s, 12 H, $-\text{CH}_2-\text{C}=\text{NOH}$), 10.49 (s, 6 H, OH). ^{13}C NMR (75 MHz, $\text{DMSO}-d_6$): $\delta = 12.1$ (CH_3), 51.1 and 52.1 ($-\text{CH}_2-\text{CH}_2-\text{N}$), 58.1 ($-\text{CH}_2-\text{C}=\text{NOH}$), 154.1 ($-\text{C}=\text{NOH}$). HRMS (micrOTOF): found 573.3814; calcd for $\text{C}_{24}\text{H}_{49}\text{N}_{10}\text{O}_6$ ($[\text{M}+\text{H}]^+$): 573.3831. FTIR, cm^{-1} : 3375s,br; 3363s,br; 3261s,br; 3125s,br; 2921s,br; 2836s,br; 1738s, sh; 1664m; 1446s,br; 1368s; 1265s,sh; 1101w; 1035s; 962s; 928s; 826w; 765w; 667m.

2.2.2. Preparation of Ox_2H_2

Ox_2H_2 was prepared from oxime **3** by a modified literature protocol [9b]. 5%–Pd/C (1.25 g) was added to a solution of bisoxime **3** (8.75 g, 35.1 mmol) in 120 mL of MeOH. The mixture was hydrogenated at 5 bar of H_2 and 50–55 °C for 1.5 h in a steel autoclave. Then the autoclave was slowly depressurized and the catalyst was filtered off. The solvent was evaporated in vacuum and the residue was crystallized from ethyl acetate/hexane mixture to give 4.13 g of Ox_2H_2 as white solid. Yield: 74%. ^1H NMR spectra of Ox_2H_2 is consistent with literature data [9b]. FTIR, cm^{-1} : 3303s; 3277s; 3186s,br; 3096s,br; 2927s; 2846s,br; 2688s,br; 1777w,br; 1657m; 1468s,sh; 1363s; 1256w; 1238m; 1210m; 1123m; 1093m; 1022s; 961s,sh; 937s; 902s; 862s,sh; 679m; 650m; 533w.

Scheme 1. Synthesis of ligands Ox_nH_n.

2.2.3. Preparation of Ni(Ox₁H₁)₂Cl₂

To NiCl₂·6H₂O (0.135 g, 0.567 mmol) was added 2.0 mL of MeOH followed by a solution of oxime Ox₁H₁ (0.100 g, 1.136 mmol) in 1.0 mL of MeOH. After 30 min of stirring the resulting green solution was left for slow evaporation at room temperature. The formed blue crystals of Ni(Ox₁H₁)₂Cl₂ (0.141 g) were collected from the residual solution (crystals suitable for X-ray crystallography were also collected) and dried in vacuum. Yield: 81%. Decomposition 190 °C. Elemental Anal. Calc. for C₆H₁₆Cl₂N₄NiO₂: C, 23.56; H, 5.27; N, 18.32. Found: C, 23.70; H, 5.66; N, 17.95%. FTIR, cm⁻¹: 3396s,br; 3301s; 3265s; 3179s,br; 2918m; 1602m,sh; 1458s; 1407m; 1306w; 1242m; 1185w; 1119m; 1054s; 1017s; 842w; 687m; 662m; 591w. UV-Vis, nm (MeOH, c = 0.01 M): 959w; 605s; 416m; 312s.

2.2.4. Preparation of Ni(Ox₂H₂)₂Cl₂

To a mixture of solid oxime Ox₂H₂ (0.150 g, 0.943 mmol) and NiCl₂·6H₂O (0.112 g, 0.471 mmol) was added 9 mL of MeOH. The resulting suspension was refluxed for 1 h and then cooled to 0 °C. The precipitate was filtered off and dried in vacuum to give 0.137 g of Ni(Ox₂H₂)₂Cl₂ as pink solid. Yield: 65%. Crystals suitable for X-ray crystallography were obtained by recrystallization from MeOH/H₂O mixture. Decomposition 230 °C. Elemental Anal. Calc. for C₁₂H₂₆Cl₂N₆NiO₄: C, 32.17; H, 5.85; N, 18.76. Found: C, 32.14; H, 6.00; N, 18.74%. HRMS (microTOF): found 375.1278; calcd for C₁₂H₂₅N₆NiO₄ ([Ni(Ox₂H₂)(Ox₂H₁)]⁺): 375.1285. FTIR, cm⁻¹: 3431s,br; 3207s,br; 3054s,br; 2935m,sh; 2815s; 1681m; 1614m,br; 1451s; 1374m; 1242m; 1232m; 1094s; 1063s; 1024m; 989m; 954s; 901w; 697s; 672s. UV-Vis, nm (DMSO, c = 0.01 M): 922w; 795w; 495w; 264s.

2.2.5. Preparation of Ni(Ox₄H₄)Cl₂(H₂O)₂

To a mixture of solid oxime Ox₄H₄ (0.147 g, 0.427 mmol) and NiCl₂·6H₂O (0.102 g, 0.427 mmol) was added 3 mL of MeOH upon intensive stirring. The resulting violet solution was left for slow isothermal evaporation at room temperature. The resulting violet solid was washed with ethyl acetate and dried in vacuum. The solid was dissolved in water (3 mL) and left for slow isothermal evaporation at room temperature to give 0.170 g of Ni(Ox₄H₄)Cl₂(H₂O)₂ as small violet needle crystals. Yield: 75%. Decomposition 250 °C. Elemental Anal. Calc. for C₁₄H₂₈Cl₂N₆NiO₄·2H₂O: C, 32.97; H, 6.32; N, 16.48. Found: C, 32.27; H, 6.30; N, 16.12%. HRMS (microTOF): found 401.1439; calcd for C₁₄H₂₇N₆NiO₄ ([Ni(Ox₄H₃)]⁺): 401.1442. FTIR, cm⁻¹: 3406s,br; 3386s,br; 3316s,br; 2928m,br; 2775s,br; 1680m,sh; 1638m,br; 1442m,sh; 1400m; 1373m; 1309w; 1247m; 1236m; 1116w; 1068m; 1037m; 996w; 928w;

861w; 660 m,br; 609m,br. UV-Vis, nm (MeOH, c = 0.02 M): 920w; 846w; 526s; 313s; 243s.

2.2.6. Preparation of Ni(Ox₆H₆)Cl₂(H₂O)₄

To a mixture of solid oxime Ox₆H₆ (0.100 g, 0.175 mmol) and NiCl₂·6H₂O (0.042 g, 0.176 mmol) was added 2 mL of MeOH. The resulting violet solution was stirred for 1 h and then the solvent was removed *via* rotary evaporation. The residue was washed with ethyl acetate, dried in vacuum, dissolved in water (2 mL) and left for slow evaporation at room temperature. The resulting pink solid was dried in vacuum to give 0.109 g of Ni(Ox₆H₆)Cl₂(H₂O)₄. Yield: 80%. Decomposition 170 °C. Elemental Anal. Calc. for C₁₄H₂₈Cl₂N₆NiO₄·4H₂O: C, 37.23; H, 7.29; N, 18.09. Found: C, 37.68; H, 6.94; N, 18.04%. HRMS (microTOF): found 629.3036; calcd for C₁₄H₂₈N₆NiO₄ ([Ni(Ox₆H₆)]²⁺): 629.3028. FTIR, cm⁻¹: 3420s,br; 3303s,br; 2921s,br; 1647s; 1474s; 1456s; 1384s,sh; 1036m,sh; 995s; 960m; 920m; 835w; 781w; 668m. UV-Vis, nm (MeOH, c = 0.02 M): 921w; 848w; 513s; 337s; 222s.

2.3. General procedure for aerobic oxidation of Ph₃P in presence of nickel complexes

In a Schlenk flask was placed Ph₃P (0.262 g, 1 mmol), nickel complex (0.2 mmol) and MeOH (12.5 mL). The resulting solution was deoxygenated by bubbling argon through it for 0.5 h. After that an appropriate amount of 1 M solution of KOH in MeOH (0.4 mL for Ni(Ox₁H₁)₂Cl₂, 0.8 mL for Ni(Ox₂H₂)₂Cl₂, 0.6 mL for Ni(Ox₃H₃)(NO₃)₂(H₂O)₂, 0.8 mL for Ni(Ox₄H₄)Cl₂(H₂O)₂, 1.2 mL for Ni(Ox₆H₆)Cl₂(H₂O)₄) was added under argon. The solution was frozen with liquid nitrogen, the flask was evacuated, connected to balloon with oxygen and allowed to warm to room temperature. Upon exposure to oxygen reactions with Ni(Ox₁H₁)₂Cl₂, Ni(Ox₂H₂)₂Cl₂ became orange, reaction with Ni(Ox₃H₃)(NO₃)₂(H₂O)₂ became brown, reaction with Ni(Ox₄H₄)Cl₂(H₂O)₂ became pink, in reaction with Ni(Ox₆H₆)Cl₂(H₂O)₄ became pink, in reaction with Ni(Ox₄H₄)Cl₂(H₂O)₂ pink precipitate formed (for changes in UV-Vis spectra of reaction mixtures see [Supporting information](#)). Reactions were stirred for 72 h at r.t. (after 48 h all mixtures became dark brown in color) and then evaporated in vacuum. The residue was preadsorbed on silica gel and subjected to a column chromatography on silica gel (eluent: ethyl acetate/hexane = 1:3 → 1:1 → 1:0). The yields of Ph₃PO are given in [Table 1](#).

2.4. X-ray crystallography

X-ray diffraction studies of single crystals of the complexes Ni(Ox₁H₁)₂Cl₂, Ni(Ox₂H₂)₂Cl₂ and Ni(Ox₄H₄)Cl₂(H₂O)₂ were

Table 1Crystal data and structure refinement parameters for Ni(Ox₁H₁)₂Cl₂, Ni(Ox₂H₂)₂Cl₂ and Ni(Ox₄H₄)Cl₂(H₂O)₂.

	Ni(Ox ₁ H ₁) ₂ Cl ₂	Ni(Ox ₂ H ₂) ₂ Cl ₂	Ni(Ox ₄ H ₄)Cl ₂ (H ₂ O) ₂
Formula	C ₆ H ₁₆ Cl ₂ N ₄ NiO ₂	C ₁₂ H ₂₆ Cl ₂ N ₆ NiO ₄	C ₂₈ H ₆₄ Cl ₄ N ₁₂ Ni ₂ O ₁₂
Molecular weight	305.84	448.00	1020.09
<i>T</i>	100	100	100
Crystal system	orthorhombic	monoclinic	triclinic
Space group	<i>Pbcn</i>	<i>P2₁/n</i>	<i>P1</i>
<i>a</i> (Å)	12.7187(7)	8.2863(9)	9.923(3)
<i>b</i> (Å)	6.4005(3)	8.9240(9)	12.987(4)
<i>c</i> (Å)	14.3134(7)	13.2155(14)	18.262(6)
α (°)	90	90	100.235(6)
β (°)	90	102.998 (2)	97.251(6)
γ (°)	90	90	101.308(5)
<i>V</i> (Å ³)	1165.2(1)	952.21(17)	2239.1(13)
<i>Z</i>	4	2	2
<i>D</i> _{calc} (g/cm ³)	1.743	1.563	1.513
Final <i>R</i> indices (<i>I</i> > 2σ(<i>I</i>))			
<i>R</i> ₁	0.0198	0.0324	0.0978
<i>wR</i> ₂	0.0493	0.0678	0.2458
<i>R</i> indices (all data)			
<i>R</i> ₁	0.0245	0.0424	0.1368
<i>wR</i> ₂	0.0521	0.0716	0.2637

performed on Bruker APEX II CCD diffractometer (Mo K α radiation, graphite monochromator). Data were collected within $1.5 < \theta < 30^\circ$ using the ω -scan method and were corrected for Lorentz-polarization effects and absorption effects (semi-empirical correction from equivalents; transmission coefficients: minimum 0.631, 0.741 and 0.687, maximum 0.690, 0.816 and 0.949, respectively) using the SADABS package [14a]. The structures were solved by direct method and were further refined by least-squares routine against F^2_{hkl} in anisotropic full-matrix approximation. All calculations were performed using SHELXTL PLUS 5.0 software [14b]. Crystal data and structure refinement parameters are listed in the Table 1. Selected bond lengths and angles for obtained complexes are presented in Table 2.

3. Results and discussion

3.1. Synthesis of ligands Ox_{*n*}H_{*n*}

Previously, the synthesis of β -oximinoalkylamine ligands Ox_{*n*}H_{*n*} (*n* = 1–6) was a rather complicated task.¹ Our group, however, recently introduced a general strategy for the assembly of poly(β -oximinoalkyl)amines of different structure via silylation of aliphatic nitro compounds [9]. According to this strategy, a general precursor of target ligands Ox₁H₁, Ox₂H₂, Ox₄H₄ and Ox₆H₆ is the commercially available 2-nitropropane (Scheme 1, see Section 2.2). This reagent is transformed by double silylation into bis(oxy)enamine **1** [10], which was then reacted with corresponding *N*-nucleophiles to give target ligands or their close precursors (Scheme 1).

Thus, for the synthesis of mono-oxime Ox₁H₁ bis(oxy)enamine **1** was initially transformed into α -azido-oxime **2** according to our previously developed procedure [12a] (Scheme 1, Eq. (1)). Subsequent selective catalytic hydrogenation of azido group furnished the desired α -amino-oxime Ox₁H₁ [12b]. Synthesis of bis-oxime Ox₂H₂ was achieved by the hydrogenolysis of its *N*-benzyl derivative **3**. The later was obtained by addition of two equivalents of bis(oxy)enamine **1** to benzylamine (Scheme 1, Eq. (2)) [9b]. Ligands

¹ Conventional methods of β -oximinoalkylamine synthesis involve the generation of highly reactive and easily polymerizable nitroso-alkenes, which results in low yields of final products and complicated procedures of their isolation [6,9a].

Ox₄H₄ and Ox₆H₆ were synthesized in one stage by addition of the required number of β -oximinoalkyl residues to ethylenediamine and tris(aminoethyl)amine (tren), respectively (Scheme 1, equations (3) and (4)). For oximes Ox₁H₁, Ox₂H₂, Ox₄H₄ and Ox₆H₆, the isomer having *E*-configuration of all oxime groups was found to be predominant. Assignment of C=N bond stereochemistry was made on the basis of known relations between the chemical shift of atoms attached to oxime group and its configuration (for example, see [9b]).

3.2. Synthesis and structure of Ox_{*n*}H_{*n*} nickel complexes

The obtained ligands Ox₁H₁, Ox₂H₂, Ox₄H₄ and Ox₆H₆ were reacted with NiCl₂ in methanol to give the corresponding complexes (yields 81%, 65%, 75% and 80%, respectively). The composition of complexes was determined by elemental analysis and high-resolution mass spectrometry (micrOTOF). The structure of nickel complexes with Ox₁H₁, Ox₂H₂ and Ox₄H₄ was established by X-ray crystallography (Figs. 3–5, Tables 1 and 2). Additional information on the structure of the complexes synthesized was obtained from FTIR spectroscopy data.

Reaction of mono-oxime Ox₁H₁ with NiCl₂ gives a blue complex Ni(Ox₁H₁)₂Cl₂. According to X-ray crystallography data, this complex has a C₂-symmetrical six-coordinated pseudo-octahedral geometry. Nickel atom is coordinated by nitrogen atoms of amino and oxime groups; the other two sites in the coordination sphere of nickel are occupied by chlorine atoms, which are *cis* to one another (Fig. 3). The equatorial plane of the complex hardly shows any distortions; the largest deviation of atoms from the mean plane Ni(1)Cl(1')N(1)N(1')N(2') does not exceed 0.03 Å. The *cis*-angle Cl(1)Ni(1)Cl(1') value in octahedron is 92.63(1)°. Similarly, Cl(1)Ni(1)N(1') and Cl(1)Ni(1)N(2') *cis*-angles are also close to 90° (86.20(3)° and 90.64(3)°, respectively), which is in line with the formation of intramolecular O–H...Cl hydrogen bonds (O...Cl 2.9988(11) Å, O–H–Cl angle 154(2)°) being an additional factor stabilizing the pseudo-octahedral geometry of the complex (Fig. 3). At the same time, the *cis*-angle N(1)Ni(1)N(2') is significantly smaller (77.79(4)°) due to the chelate ring formation that leads to the increase of the *cis*-angle N(1)Ni(1)N(2) up to 101.21(4)°.

In Ni(Ox₁H₁)₂Cl₂, chelate rings are characterized by twist conformation with atoms C(2) and N(2') going out from the mean plane defined by all five atoms of the chelate ring on –0.137(2) and 0.138(2) Å, respectively. In chelate rings, distances between nickel and oxime nitrogens are shorter than Ni–N (amine) ones (see data in Table 2). A similar tendency is observed in previously reported nickel complexes with Ox₃H₃ [13].

The major motif of Ni(Ox₁H₁)₂Cl₂ crystal lattice is an infinite chain in which molecules of the complex are assembled by moderate hydrogen bonds N–H...Cl (N...Cl 3.297(1) Å, angle N–H–Cl 146.5(2)°, Fig. 6A). These chains form layers by means of strong O...O interactions between oxime groups (O...O 2.728(1) Å, Fig. 6B). Analysis of Cambridge Structural Database [14c] showed that such intramolecular interactions are quite often observed in structures in which O–H fragment of oxime group is involved in hydrogen bonding. The formation of a 3D-framework is completed by means of weak interactions between the above-mentioned layers, i.e. hydrogen bonds N–H...Cl (N...Cl 3.368(1) Å, angle N–H–Cl 141.4(1)°).

Note that nickel complexes with α -amino-oximes like Ox₁H₁ are virtually unknown. In contrast to Ni(Ox₁H₁)₂Cl₂, the only known complex of this type with 3-amino-3-methyl-2-butanone oxime as a ligand has a square-planar structure (Fig. 7) [15].

Similarly to the complex Ox₁H₁, bis-oxime Ox₂H₂ produces a pink complex with nickel to ligand ratio 1:2. The centrosymmetric complex Ni(Ox₂H₂)₂Cl₂ is characterized by a six-coordinated pseudo-octahedral geometry (Fig. 4), with all coordination positions

Table 2
Selected bond lengths and angles^a for the complexes Ni(Ox₁H₁)₂Cl₂, Ni(Ox₂H₂)₂Cl₂ and Ni(Ox₄H₄)Cl₂(H₂O)₂.

Complex	Ni(Ox ₁ H ₁) ₂ Cl ₂	Ni(Ox ₂ H ₂) ₂ Cl ₂	Ni(Ox ₄ H ₄)Cl ₂ (H ₂ O) ₂	
			Ni(Ox ₄ H ₄)Cl ₂	[Ni(Ox ₄ H ₄)Cl]Cl
Ni–N(oxime) (Å)	Ni(1)–N(1)	Ni(1)–N(1)	Ni(1)–N(1)	Ni(1A)–N(1A)
	2.056(1)	2.068(2)	2.127(6)	2.064(7)
		Ni(1)–N(3)	Ni(1)–N(2)	Ni(1A)–N(4A)
		2.064(1)	2.097(6)	2.026(6)
			Ni(1)–N(4)	Ni(1A)–N(5A)
		2.096(6)	2.061(6)	
		Ni(1)–N(5)		
		2.060(6)		
Ni–N(amine) (Å)	Ni(1)–N(2)	Ni(1)–N(2)	Ni(1)–N(3)	Ni(1A)–N(3A)
	2.099(1)	2.110(1)	2.111(6)	2.115(6)
			Ni(1)–N(6)	Ni(1A)–N(6A)
		2.101(6)	2.187(6)	
Ni–Cl, Å	Ni(1)–Cl(1)	–	–	Ni(1A)–Cl(1A)
	2.4647(3)			2.369(2)
Angles in octahedron, (°)	Cl(1)–Ni(1)–N(1)	N(1)–Ni(1)–N(2')	N(5)–Ni(1)–N(4)	N(4A)–Ni(1A)–N(5A)
	94.77(3)	79.52(5)	89.0(2)	171.2(2)
	Cl(1)–Ni(1)–N(2')	N(1)–Ni(1)–N(3)	N(5)–Ni(1)–N(2)	N(4A)–Ni(1A)–N(1A)
	90.64(3)	88.84(6)	173.3(2)	93.5(2)
	Cl(1)–Ni(1)–Cl(1')	N(1)–Ni(1)–N(2)	N(4)–Ni(1)–N(2)	N(5A)–Ni(1A)–N(1A)
	92.63(1)	100.48(5)	92.5(2)	93.1(2)
	Cl(1)–Ni(1)–N(1')	N(1)–Ni(1)–N(3')	N(5)–Ni(1)–N(6)	N(4A)–Ni(1A)–N(3A)
	86.20(3)	91.16(6)	79.4(2)	80.9(2)
	Cl(1)–Ni(1)–N(2)	N(2)–Ni(1)–N(2')	N(4)–Ni(1)–N(6)	N(5A)–Ni(1A)–N(3A)
	163.87(3)	180	78.4(2)	94.8(2)
	N(1)–Ni(1)–N(2')	N(2)–Ni(1)–N(3')	N(2)–Ni(1)–N(6)	N(1A)–Ni(1A)–N(3A)
	77.79(4)	100.61(6)	94.5(2)	78.1(2)
	N(1)–Ni(1)–N(1')	N(2)–Ni(1)–N(3')	N(5)–Ni(1)–N(3)	N(4A)–Ni(1A)–N(6A)
	178.60(4)	79.39(6)	96.1(2)	92.0(2)
	N(1)–Ni(1)–N(2)		N(4)–Ni(1)–N(3)	N(5A)–Ni(1A)–N(6A)
	101.21(4)		162.3(2)	79.9(2)
	N(2)–Ni(1)–N(2')		N(2)–Ni(1)–N(3)	N(1A)–Ni(1A)–N(6A)
	90.59(4)		80.7(2)	161.2(2)
			N(6)–Ni(1)–N(3)	N(3A)–Ni(1A)–N(6A)
			85.8(2)	85.1(2)
		N(5)–Ni(1)–N(1)	N(4A)–Ni(1A)–Cl(1A)	
		89.8(2)	90.41(17)	
		N(4)–Ni(1)–N(1)	N(5A)–Ni(1A)–Cl(1A)	
		119.8(2)	94.74(19)	
		N(2)–Ni(1)–N(1)	N(1A)–Ni(1A)–Cl(1A)	
		95.1(2)	95.47(17)	
		N(6)–Ni(1)–N(1)	N(3A)–Ni(1A)–Cl(1A)	
		159.0(2)	168.75(17)	
		N(3)–Ni(1)–N(1)	N(6A)–Ni(1A)–Cl(1A)	
		77.4(2)	102.40(16)	

^a The atoms labeled with an asterisk in the case of the complexes Ni(Ox₁H₁)₂Cl₂ and Ni(Ox₂H₂)₂Cl₂ were obtained from the basic ones by the symmetry operations $-x, +y, 0.5 - z$ and $-x + 1, -y + 1, -z + 1$, respectively.

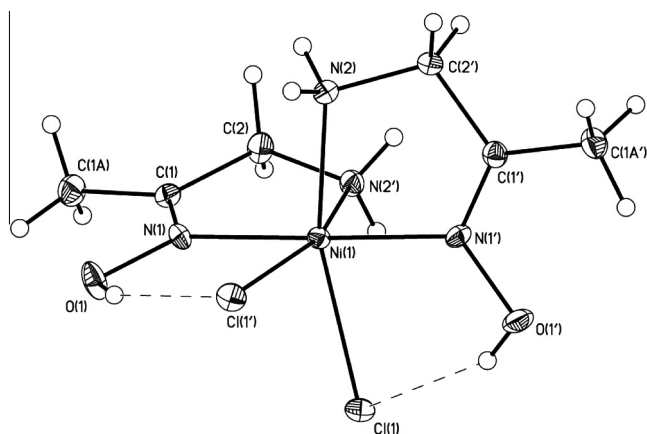


Fig. 3. Molecular structure (X-ray) and atom numbering for Ni(Ox₁H₁)₂Cl₂. All non-hydrogen atoms are represented by probability ellipsoids of atomic displacements ($p = 50\%$).

occupied by nitrogen atoms of both ligands. The equatorial plane Ni(1)N(1)N(1')N(2)N(2') of the complex does not show any pronounced distortions. The largest deviation of the N–Ni–N angles from 90° is observed for the *cis*-angle N(1)Ni(1)N(2) that is equal to 100.48(5)°; the values of the angles N–Ni–N in chelate rings being around 79.5° (Table 2). The chelate rings are characterized by an envelope conformation with the atom Ni(1) deviating by 0.489(2) Å from the mean plane defined by other four atoms. Similar to the complex Ni(Ox₁H₁)₂Cl₂, distances between nickel and oxime nitrogen atoms in Ni(Ox₂H₂)₂Cl₂ are shorter than Ni–N(amine) ones (see Table 2).

Chloride anions are involved in hydrogen bonding with NH-group and two OH-groups of ligands Ox₂H₂. Distances N···Cl and O···Cl are 3.279(2), 3.029(2) and 2.999(1) Å, respectively. Formation of hydrogen bonds between counterion and oxime OH-groups was observed in some other nickel complexes with β-oximinoalkyl ligands [11,13].

Baldwin and coauthors reported the synthesis and structure characterization of more than ten Ni(II) complexes with various bis(oximinoalkyl)amines RN[CH₂C(NO)CH₃]₂ having a substituent

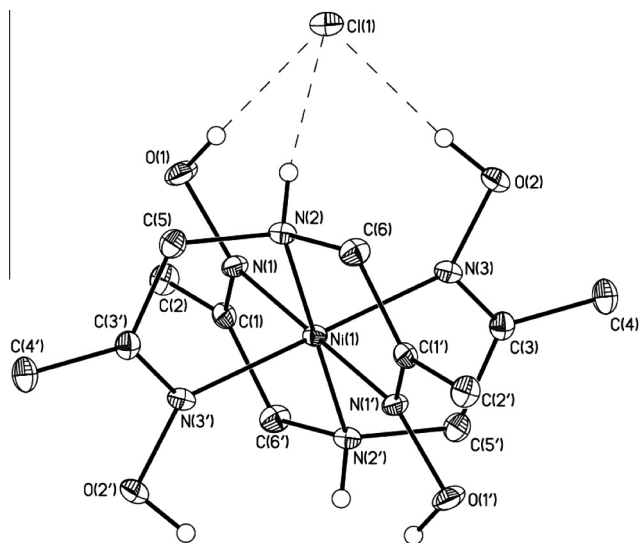


Fig. 4. Molecular structure (X-ray) and atom numbering for $\text{Ni}(\text{Ox}_2\text{H}_2)_2\text{Cl}_2$. The H(C) hydrogen atoms and Cl(2) are omitted for clarity. All non-hydrogen atoms are represented by probability ellipsoids of atomic displacements ($p = 50\%$).

R (alkyl, aryl, phenethyl group) at sp^3 nitrogen atom [11]. In none of these complexes, however, coordination of nickel atom by two ligands was observed. In contrast to $\text{Ni}(\text{Ox}_2\text{H}_2)_2\text{Cl}_2$, all previously reported complexes of this type have nickel to ligand ratio 1:1. Presumably, this is due to steric hindrances created by substituent R in N-substituted derivatives of Ox_2H_2 . Thus, $\text{Ni}(\text{Ox}_2\text{H}_2)_2\text{Cl}_2$ can be considered as a novel structural type for β -oximinoalkylamine nickel complexes.

Violet-colored Ni(II) complex of tetraoxime Ox_4H_4 was much harder to crystallize from the solution compared to the complexes $\text{Ni}(\text{Ox}_1\text{H}_1)_2\text{Cl}_2$ and $\text{Ni}(\text{Ox}_2\text{H}_2)_2\text{Cl}_2$. Single crystal X-ray diffraction study of $\text{Ni}(\text{Ox}_4\text{H}_4)\text{Cl}_2(\text{H}_2\text{O})_2$ showed the presence of two independent complex cations $[\text{Ni}(\text{Ox}_4\text{H}_4)]^{2+}$ and $[\text{Ni}(\text{Ox}_4\text{H}_4)\text{Cl}]^+$, three chloride anions and four water molecules (Fig. 5). In the first cation, nickel atom is coordinated to all nitrogen atoms of ligand Ox_4H_4 (sp^3 nitrogen atoms are located in *cis*-positions in the coordination octahedron). In the second complex cation, one of the oxime groups is not bounded to nickel atom, and chlorine atom occupies the sixth coordination position in the octahedron. It is likely that there is an equilibrium between cations $[\text{Ni}(\text{Ox}_4\text{H}_4)]^{2+}$ and $[\text{Ni}(\text{Ox}_4\text{H}_4)\text{Cl}]^+$ in solution (Scheme 2).

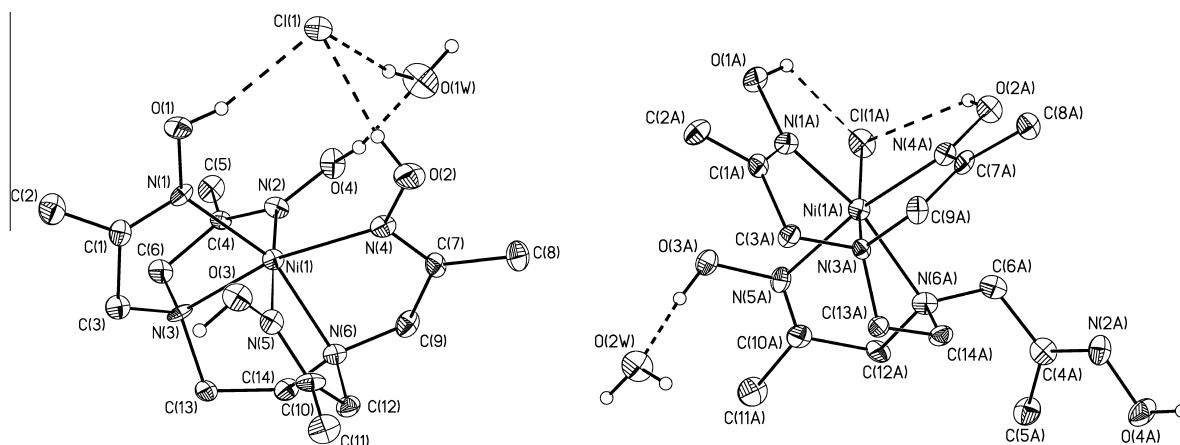


Fig. 5. General view (X-ray) and atom numbering of two independent species $\text{Ni}(\text{Ox}_4\text{H}_4)\text{Cl}(\text{H}_2\text{O})$ in a crystal of $\text{Ni}(\text{Ox}_4\text{H}_4)\text{Cl}_2(\text{H}_2\text{O})_2$. H(C) hydrogen atoms are omitted for clarity. All non-hydrogen atoms are represented by probability ellipsoids of atomic displacements ($p = 50\%$).

The structure of the complex cation $[\text{Ni}(\text{Ox}_4\text{H}_4)]^{2+}$ is similar to that of $[\text{Ni}(\text{Ox}_2\text{H}_2)_2]^{2+}$ with the difference that two amino groups of ligands are tethered by 1,2-ethylene bridge. This leads to a noticeable distortion of the octahedral configuration of nickel (the largest deviation from the mean equatorial plane $\text{Ni}(1)\text{N}(1)\text{N}(3)\text{N}(4)\text{N}(6)$ is $0.19(1)\text{ \AA}$). Furthermore, amino groups are located *cis* to one another, whereas in $[\text{Ni}(\text{Ox}_2\text{H}_2)_2]^{2+}$ amino groups occupy *trans*-positions. Interestingly, three of four bonds between nickel and oxime nitrogen atoms in the complex $[\text{Ni}(\text{Ox}_4\text{H}_4)]^{2+}$ are slightly elongated compared to $\text{Ni}(\text{Ox}_1\text{H}_1)_2\text{Cl}_2$, $[\text{Ni}(\text{Ox}_2\text{H}_2)_2]^{2+}$ and $[\text{Ni}(\text{Ox}_4\text{H}_4)\text{Cl}]^+$ (cf. data in Table 2). Apparently, this lengthening is due to a strain in $[\text{Ni}(\text{Ox}_4\text{H}_4)]^{2+}$ structure possessing five chelate rings. As it can be seen from Table 2, opening of one of five-membered chelate rings with a chloride anion that forms $[\text{Ni}(\text{Ox}_4\text{H}_4)\text{Cl}]^+$ species relieves the chelate strain (Scheme 2).

Most of N–Ni–N angles in the octahedron $[\text{Ni}(\text{Ox}_4\text{H}_4)]^{2+}$ are distorted due to the formation of chelate rings. Thus, angles $\text{N}(1)\text{Ni}(1)\text{N}(3)$, $\text{N}(2)\text{Ni}(1)\text{N}(3)$, $\text{N}(5)\text{Ni}(1)\text{N}(6)$ and $\text{N}(4)\text{Ni}(1)\text{N}(6)$ (chelate rings involving nitrogen atoms of amino group and oxime group) are $77.4(2)^\circ$, $80.7(2)^\circ$, $79.4(2)^\circ$ and $78.4(2)^\circ$, respectively; angle $\text{N}(3)\text{Ni}(1)\text{N}(6)$ in chelate ring involving two nitrogen atoms of amino groups (Fig. 5) is $85.8(2)^\circ$, the *cis*-angle $\text{N}(1)\text{Ni}(1)\text{N}(4)$ is $119.8(2)^\circ$. Nitrogen atoms $\text{N}(2)$ and $\text{N}(5)$ of coordinated oxime groups are practically perpendicular to the equatorial plane $\text{Ni}(1)\text{N}(1)\text{N}(3)\text{N}(4)\text{N}(6)$.

Chelate rings in this equatorial plane (rings $\text{Ni}(1)\text{N}(1)\text{C}(1)\text{C}(3)\text{N}(3)$, $\text{Ni}(1)\text{N}(3)\text{C}(13)\text{C}(14)\text{N}(6)$ and $\text{Ni}(1)\text{N}(4)\text{C}(7)\text{C}(9)\text{N}(6)$) are characterized by a twist conformation: in these cases, the atoms that deviate the most are N3 and C3 (by $-0.96(1)$ and $0.32(1)\text{ \AA}$); C(13) and C(14) (by $-0.27(1)$ and $0.46(1)\text{ \AA}$), N(6) and C(9) (by $-0.59(1)$ and $-0.12(1)\text{ \AA}$). Chelate rings that are perpendicular to the equatorial plane $\text{Ni}(1)\text{N}(1)\text{N}(3)\text{N}(4)\text{N}(6)$ are more planar with the largest deviation of an atom from the mean plane equal to $0.07(1)\text{ \AA}$.

One of chloride anions is involved in hydrogen bonding $\text{O}\cdots\text{H}\cdots\text{Cl}$ with hydroxyl groups of two coordinated oxime fragments of $[\text{Ni}(\text{Ox}_4\text{H}_4)]^{2+}$ cation ($\text{O}\cdots\text{Cl}$ $3.060(6)$ and $3.086(6)\text{ \AA}$, OHCl $156(1)^\circ$ and $164(1)^\circ$); O–H group of third oxime fragment is bound to one of the solvate water molecules ($\text{O}\cdots\text{O}$ $2.618(8)\text{ \AA}$, OHO $155(1)^\circ$).

The second complex cation $[\text{Ni}(\text{Ox}_4\text{H}_4)\text{Cl}]^+$ has a pseudo-octahedral structure with a distorted equatorial plane $\text{Ni}(1\text{A})\text{Cl}(1\text{A})\text{N}(1\text{A})\text{N}(3\text{A})\text{N}(6\text{A})$; the largest deviation of these atoms from the mean plane reaches $0.18(1)\text{ \AA}$. Geometrical parameters of chelate rings in $[\text{Ni}(\text{Ox}_4\text{H}_4)\text{Cl}]^+$ are quite similar to those in the cation $[\text{Ni}(\text{Ox}_4\text{H}_4)]^{2+}$. Formation of chelate rings results in a distortion of

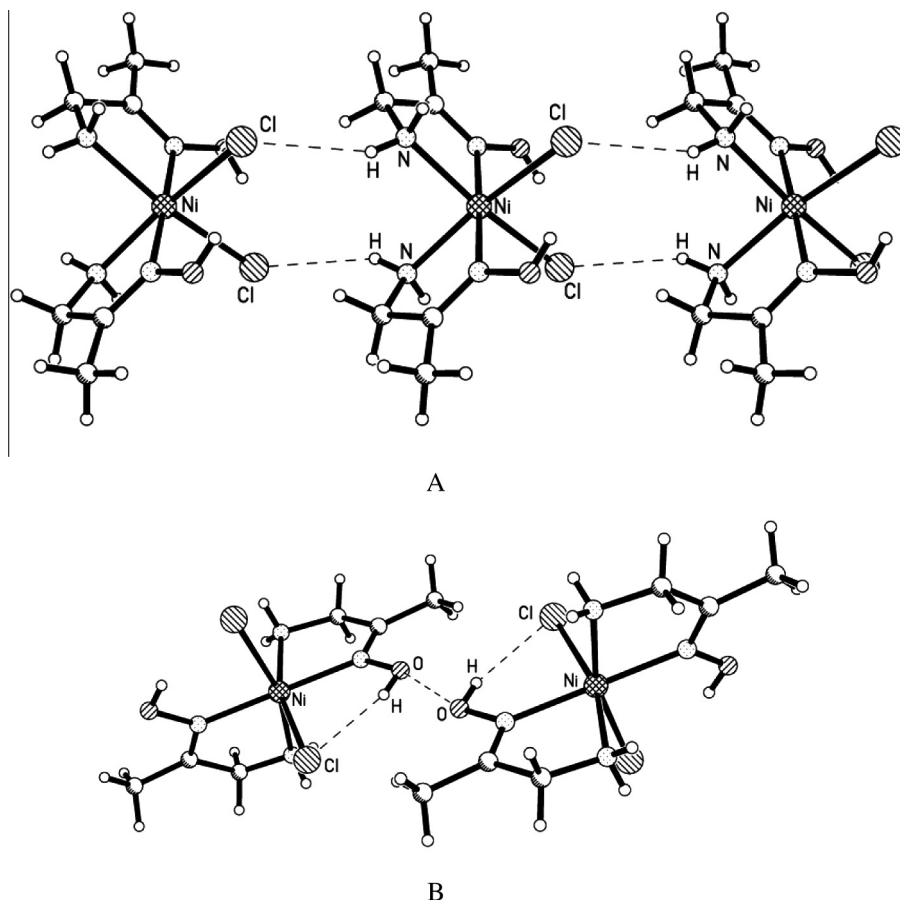


Fig. 6. Fragments of crystal packing of the complex $\text{Ni}(\text{Ox}_4\text{H}_4)_2\text{Cl}_2$ representing H-bonded chains (A) and the intermolecular $\text{O}\cdots\text{O}$ interaction between the oxime groups (B).

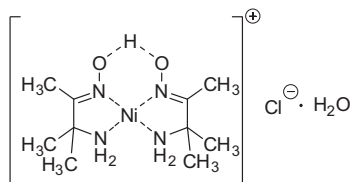
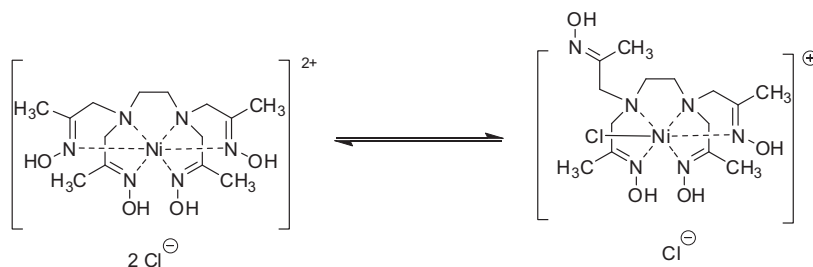


Fig. 7. Nickel complex of 3-amino-3-methyl-2-butanone oxime.

octahedron angles. Thus, the angle $\text{Cl}(1\text{A})\text{Ni}(1\text{A})\text{N}(1\text{A})(\text{oxime})$ is $95.47(17)^\circ$, angle $\text{Cl}(1\text{A})\text{Ni}(1\text{A})\text{N}(6\text{A})(\text{oxime})$ is $102.40(16)^\circ$. Nitrogen atoms $\text{N}(4\text{A})$ and $\text{N}(5\text{A})$ of coordinated oxime fragments are practically perpendicular to the equatorial plane $\text{Ni}(1\text{A})\text{Cl}(1\text{A})\text{N}(1\text{A})\text{N}(3\text{A})\text{N}(6\text{A})$. Similar to $[\text{Ni}(\text{Ox}_4\text{H}_4)]^{2+}$, the geometry of the cation $[\text{Ni}(\text{Ox}_4\text{H}_4)\text{Cl}]^+$ is additionally stabilized by two $\text{O}\cdots\text{H}\cdots\text{Cl}$ bonds between oximine hydroxyl groups and a coordinated chlorine atom, although they are much weaker in this case ($\text{O}\cdots\text{Cl}$

$3.148(6)$ and $3.380(6)$ Å, angles OHCl are $130(1)^\circ$ and $139(1)^\circ$, respectively).

The crystal structure of $\text{Ni}(\text{Ox}_4\text{H}_4)\text{Cl}_2(\text{H}_2\text{O})_2$ displays a complex system of hydrogen bonds between OH-groups of oxime fragments, molecules of water and chloride anions. The independent complex species $[\text{Ni}(\text{Ox}_4\text{H}_4)]^{2+}$ and $[\text{Ni}(\text{Ox}_4\text{H}_4)\text{Cl}]^+$ are held together by a rather weak $\text{O}\cdots\text{H}\cdots\text{O}$ bond between oxygen atoms of their oxime hydroxyl groups ($\text{O}\cdots\text{O}$ $2.854(7)$ Å, angle OHO is $129(1)^\circ$), through hydrogen bonding of hydroxyl groups with solvate water molecules ($\text{O}\cdots\text{O}$ $2.596(8)$ – $2.941(9)$ Å, angle OHO $107(1)$ – $173(1)^\circ$), with free chloride anions ($\text{O}\cdots\text{Cl}$ $3.003(6)$ Å, OHCl $178(1)^\circ$) and between chloride anions and water molecules ($\text{O}\cdots\text{Cl}$ $3.067(6)$ – $3.259(12)$ Å, angle OHCl $158(1)$ – $170(1)^\circ$). The formation of a 3D-framework is completed by a $\text{O}\cdots\text{H}(\text{water})\cdots\text{N}$ bond involving a non-coordinated oxime nitrogen atom $\text{N}(2\text{A})$ ($\text{O}\cdots\text{N}$ $2.823(9)$ Å, OHN $152(1)^\circ$) and an additional interaction between solvate water molecules ($\text{O}\cdots\text{O}$ $3.106(13)$ Å, OHO $149(1)^\circ$).



Scheme 2. Equilibrium between $\text{Ni}(\text{Ox}_4\text{H}_4)\text{Cl}_2$ and $[\text{Ni}(\text{Ox}_4\text{H}_4)\text{Cl}]\text{Cl}$.

Interaction of hexa-oxime ligand Ox_6H_6 with NiCl_2 in equimolar amounts produced a violet complex $\text{Ni}(\text{Ox}_6\text{H}_6)\text{Cl}_2(\text{H}_2\text{O})_4$ according to elemental analysis data. In high-resolution mass spectra (micro-TOF, electrospray ionization), only one ion ($m = 629.3036$) corresponding to $\text{Ni}(\text{Ox}_6\text{H}_6)^{2+}$ ($|\delta| = 1.2$ ppm) was observed. Unfortunately, crystals of the complex suitable for X-ray crystallography could not be obtained. Changing of counterion to perchlorate also did not furnish the crystalline complex. In HRMS spectra of perchlorate complex, only ion $\text{Ni}(\text{Ox}_6\text{H}_6)^{2+}$ (629.3011 , $|\delta| = 2.7$ ppm) was detected as well. This indicates that in the complex $\text{Ni}(\text{Ox}_6\text{H}_6)\text{Cl}_2(\text{H}_2\text{O})_4$ nickel atom is coordinated only by nitrogen atoms of the ligand with chlorine atoms located out of the metal's coordination sphere. Reaction of hexa-oxime Ox_6H_6 with two equivalents of nickel perchlorate does not furnish the dinuclear complex, though several non-coordinated donor groups should be present in $\text{Ni}(\text{Ox}_6\text{H}_6)^{2+}$ cation (for the synthesis of dinuclear nickel complexes with some β -oximinoalkylamine ligands see Ref. [16]). In HRMS spectra of the resulting product, only ion of mononuclear complex $\text{Ni}(\text{Ox}_6\text{H}_6)^{2+}$ (629.3028 , $|\delta| = 0$ ppm) was observed.

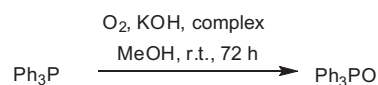
In FTIR spectra of the complexes $\text{Ni}(\text{Ox}_1\text{H}_1)_2\text{Cl}_2$, $[\text{Ni}(\text{Ox}_2\text{H}_2)_2]\text{Cl}_2$, $\text{Ni}(\text{Ox}_4\text{H}_4)\text{Cl}_2(\text{H}_2\text{O})_2$ and $\text{Ni}(\text{Ox}_6\text{H}_6)\text{Cl}_2(\text{H}_2\text{O})_4$, characteristic bands corresponding to oxime fragments are present, i.e. broad bands at $3400\text{--}3600\text{ cm}^{-1}$ (O–H bond stretch), $1600\text{--}1700\text{ cm}^{-1}$ (C=N bond stretch), $950\text{--}1100\text{ cm}^{-1}$ (N–O bond stretch) and characteristic bands of C–N bond stretch in $1210\text{--}1250\text{ cm}^{-1}$ region. These data are in agreement with experimental and calculated (ub3lyp) IR spectra of $\text{Ni}(\text{Ox}_3\text{H}_3)\text{Cl}_2$, which is the most structurally related to the obtained complexes [13a]. In nickel complexes of Ox_4H_4 and Ox_6H_6 , several bands in region $1600\text{--}1700\text{ cm}^{-1}$ are observed, which presumably correspond to a coordinated and non-coordinated oxime C=N bond stretching.

Thus, in spite of significant distinctions in structures of Ox_1H_1 , Ox_2H_2 , Ox_3H_3 , Ox_4H_4 and Ox_6H_6 nickel complexes, the metal–ligand complexation in these series shares some general features. First, all Ox_nH_n complexes have a six-coordinated pseudo-octahedral structure. Second, ligands Ox_nH_n coordinate nickel by both amino group's and oxime groups' nitrogen atoms forming five-membered chelate rings, which have similar geometrical parameters for all considered ligands. Third, OH-groups of coordinated oxime fragments are involved in hydrogen bonding with counterions (Cl^-), which can be located in the inner or outer coordination sphere of nickel. Intramolecular hydrogen bonding effects may enhance the catalytic activity due to additional stabilization of intermediate oxygen-containing species and complexes with oxidation substrate [17].

3.3. Study of oxygen reactivity of nickel complexes

Each of the obtained complexes was studied in a model oxidation reaction of triphenylphosphine in molecular oxygen atmosphere in the presence of potassium hydroxide as a base (Scheme 3, Table 3). In these experiments, 5 equivalents of triphenylphosphine with respect to nickel complex were used. The amount of base (KOH) per nickel complex was taken equal to the number of NOH-fragments in a complex for an exhaustive deprotonation of all ligand's oxime groups. For comparison purposes, aerobic oxidation of Ph_3P in presence of $\text{Ni}(\text{Ox}_3\text{H}_3)(\text{NO}_3)_2(\text{H}_2\text{O})_2$ previously reported by Baldwin and co-workers [6] was performed (Table 3, entry 1).

In all cases, exposure of the solution of Ph_3P and deprotonated nickel complex to oxygen atmosphere resulted in deep color changes (up to deep-brown after 48 h of exposure, for changes in UV–Vis spectra see Supporting information). In argon atmosphere, no color change was observed. Baldwin's tris-oxime complex $\text{Ni}(\text{Ox}_3\text{H}_3)(\text{NO}_3)_2(\text{H}_2\text{O})_2$ under the studied conditions promotes oxidation of 2 equivalents of Ph_3P , which is in good agreement



Scheme 3. Aerobic oxidation of Ph_3P in presence of $\text{Ni}(\text{Ox}_n\text{H}_n)_m\text{X}_2$ complexes.

Table 3
Results of Ni(II)-promoted Ph_3P aerobic oxidation experiments.

Entry	Complex	Amount of KOH (equivalents to complex)	Yield of Ph_3PO , % ^{a,b}	N ^c
1	$\text{Ni}(\text{Ox}_3\text{H}_3)(\text{NO}_3)_2(\text{H}_2\text{O})_2$	3	41	2.05 (2.0 ^d)
2	$\text{Ni}(\text{Ox}_3\text{H}_3)(\text{NO}_3)_2(\text{H}_2\text{O})_2$	0	0 ^e	0 (0 ^d)
3	none	– ^f	0 ^g	0
4	$\text{Ni}(\text{Ox}_3\text{H}_3)\text{Cl}_2$	3	45	2.25
5	$\text{Ni}(\text{Ox}_1\text{H}_1)_2\text{Cl}_2$	2	8	0.4
6	$\text{Ni}(\text{Ox}_2\text{H}_2)_2\text{Cl}_2$	4	37	1.85
7	$\text{Ni}(\text{Ox}_4\text{H}_4)\text{Cl}_2(\text{H}_2\text{O})_2$	4	15	0.75 ^d
8	$\text{Ni}(\text{Ox}_6\text{H}_6)\text{Cl}_2(\text{H}_2\text{O})_4$	6	19	0.95
9	$\text{NiCl}_2 \cdot 6\text{H}_2\text{O}$	6	10	0.5

^a Yield of Ph_3PO isolated by flash chromatography from reaction mixture.

^b Average of two experiments.

^c N – equivalents of Ph_3PO formed per 1 equivalent of nickel complex.

^d Lit. data [6].

^e Only starting material was recovered (92%).

^f 1 Equivalent of KOH to PPh_3 was used.

^g Only starting material was recovered (99%).

with previously reported data [6] (Table 3, entry 1). In the absence of KOH, no oxidation of Ph_3P to Ph_3PO was detected (Table 3, entry 2). Similarly, in the absence of nickel complexes no oxidation of Ph_3P with dioxygen occurred, and the starting material was quantitatively recovered in this experiment (Table 3, entry 3). Another tris-oxime complex $\text{Ni}(\text{Ox}_3\text{H}_3)\text{Cl}_2$ [11] promoted Ph_3P oxidation to a similar extent as $\text{Ni}(\text{Ox}_3\text{H}_3)(\text{NO}_3)_2(\text{H}_2\text{O})_2$ did (cf. entries 1 and 4 in Table 3) demonstrating no significant counterion effect on dioxygen reactivity of nickel Ox_3H_3 complexes.²

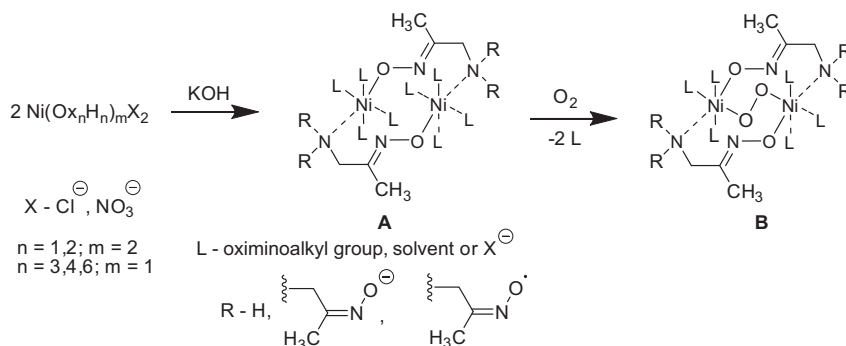
A similar activity to $\text{Ni}(\text{Ox}_3\text{H}_3)(\text{NO}_3)_2(\text{H}_2\text{O})_2$ was found for bis-oxime complex $\text{Ni}(\text{Ox}_2\text{H}_2)_2\text{Cl}_2$, which promotes formation of almost 2 equivalents Ph_3PO per 1 equivalent of complex (Table 3, entry 6). Nickel complexes of tetra-oxime Ox_4H_4 and hexa-oxime Ox_6H_6 proved to be much less active promoters leading to oxidation of less than 20% of initial triphenylphosphine (less than 1 equivalent of Ph_3PO per complex was formed, Table 3, entries 7 and 8). The lowest yield of Ph_3PO (less than 10%) was observed in Ph_3P oxidation reaction promoted by mono-oxime complex $\text{Ni}(\text{Ox}_1\text{H}_1)_2\text{Cl}_2$ (Table 3, entry 5).

Interestingly, NiCl_2 in the presence of KOH led to oxidation of Ph_3P with dioxygen, though to a small extent (yield of Ph_3PO c.a. 10%, Table 3, entry 9). Apparently, nickel hydroxide serves as a Ph_3P oxidation promoter in this reaction.³ Examples of aerobic oxidation of some organic substrates (primary and secondary alcohols) employing nickel hydroxide as heterogeneous catalyst at elevated temperatures are precedent in literature [18].

According to Baldwin's hypothesis [6,7], the ability of complex $\text{Ni}(\text{Ox}_3\text{H}_3)(\text{NO}_3)_2(\text{H}_2\text{O})_2$ to promote aerobic oxidation is governed by stabilization of Ni(III) ion by coordination with three deprotonated oximate groups (lowering the oxidation potential of Ni(II) to Ni(III) transfer) and by formation of oximate-bridged dinuclear

² Complex $\text{Ni}(\text{Ox}_3\text{H}_3)\text{Cl}_2$ was not studied for the ability to promote in aerobic oxidation reactions before.

³ Nickel hydroxide is a well-known redox-active compound. In particular, in alkaline conditions it is oxidized by strong oxidants (H_2O_2 , NaClO) to higher nickel oxides.



Scheme 4. Plausible mechanism of the reaction of complexes $\text{Ni}(\text{Ox}_n\text{H}_n)_m\text{X}_2$ with O_2 in presence of KOH.

nickel complexes **A** (Scheme 4). The latter is oxidized with dioxygen to give intermediate **B** which may also contain iminoxyl radical groups [7c] (Scheme 4). In this context, low activity of mono-oxime complex $\text{Ni}(\text{Ox}_1\text{H}_1)_2\text{Cl}_2$ may be caused by an inefficient stabilization of Ni(III) by only two oximate groups in corresponding intermediate dimers **B**. On the other hand, moderate activity of tetra-oxime and hexa-oxime complexes may be due to some difficulties in forming oximate-bridged dimers **A** associated with greater sterical hindrances of these ligands **A** compared to Ox_2H_2 and Ox_3H_3 and the presence of many donor nitrogen atoms occupying all nickel's coordination sphere. The mechanism of Ni(II)-promoted aerobic oxidation remains still ambiguous and requires further studies.

Thus, it turns to be that not only nickel complexes of Ox_3H_3 , but also complexes with other Ox_nH_n ligands ($n = 1-6$) are capable to promote aerobic oxidation of triphenylphosphine.

4. Conclusions

In conclusion, four new nickel complexes with β -oximinoalkylamine ligands Ox_nH_n containing one (Ox_1H_1), two (Ox_2H_2), four (Ox_4H_4) and six (Ox_6H_6) oxime groups were synthesized and structurally characterized. Two new structural types of octahedral oximinoalkylamine complexes of Ni(II) containing two ligands per one nickel ($\text{Ni}(\text{Ox}_1\text{H}_1)_2\text{Cl}_2$ and $\text{Ni}(\text{Ox}_2\text{H}_2)_2\text{Cl}_2$) were identified. The number of oxime groups in ligand Ox_nH_n substantially affects the structure and dioxygen reactivity of corresponding nickel complexes. The highest activity in promoting aerobic oxidation of triphenylphosphine is observed for Ni- Ox_nH_n complexes with $n = 3$ (complexes $\text{Ni}(\text{Ox}_3\text{H}_3)(\text{NO}_3)_2(\text{H}_2\text{O})_2$ [6] and $\text{Ni}(\text{Ox}_3\text{H}_3)\text{Cl}_2$) and $n = 2$ (complex $\text{Ni}(\text{Ox}_2\text{H}_2)_2\text{Cl}_2$). Nickel complexes with ligands having less (Ox_1H_1) or more (Ox_4H_4 and Ox_6H_6) oxime groups promote aerobic oxidation of triphenylphosphine to a much lesser extent.

The general algorithm for the assembly of β -oximinoalkylamines of different structure from aliphatic nitro compounds suggested by us provides vast opportunities for the rational design of the structure of ligands Ox_nH_n . This will allow one to tune the dioxygen reactivity of complexes and reveal the most active promoters of aerobic oxidation among Ni(II) coordination compounds.

Acknowledgments

The financial support from Russian President's Council for Grants (grant MK-3918.2013.3), Russian Foundation for Basic Research (#14-03-00933a) and Presidium of Russian Academy of Sciences (Program 8P) is greatly acknowledged.

Appendix A. Supplementary data

CCDC 956446–956448 contain the supplementary crystallographic data for $\text{Ni}(\text{Ox}_1\text{H}_1)_2\text{Cl}_2$, $\text{Ni}(\text{Ox}_2\text{H}_2)_2\text{Cl}_2$ and $\text{Ni}(\text{Ox}_4\text{H}_4)_2\text{Cl}_2$ ($\text{H}_2\text{O})_2$. These data can be obtained free of charge via <http://www.ccdc.cam.ac.uk/conts/retrieving.html>, or from the Cambridge Crystallographic Data Centre, 12 Union Road, Cambridge CB2 1EZ, UK; fax: +44 1223-336-033; or e-mail: deposit@ccdc.cam.ac.uk. Supplementary data associated with this article can be found, in the online version, at <http://dx.doi.org/10.1016/j.poly.2014.01.003>.

References

- (a) J.-E. Backvall (Ed.), *Modern Oxidation Methods*, Wiley-VCH, Weinheim, 2006;
 (b) M.G. Clerici, O.A. Kholdeeva (Eds.), *Liquid Phase Oxidation via Heterogeneous Catalysis: Organic Synthesis and Industrial Applications*, Wiley, Hoboken, New Jersey, 2013;
 (c) P.G. Andersson (Ed.), *Innovative Catalysis in Organic Synthesis: Oxidation: Hydrogenation and C-X Bond Forming Reactions*, Wiley-VCH, Weinheim, 2012.
- (a) W.-D. Fessner, T. Anthonsen (Eds.), *Modern Biocatalysis*, Wiley-VCH, Weinheim, 2009;
 (b) A. Messerschmidt, W. Bode, M. Cygler (Eds.), *Handbook of Metalloproteins*, vol. 3, Wiley, 2004;
 (c) A. Sigel, H. Sigel, R.K.O. Sigel (Eds.), *The Ubiquitous Roles of Cytochrome P450 Proteins: Metal Ions in Life Sciences*, vol. 3, Wiley, Chichester, 2007;
 (d) R. Lieberman, A.C. Rosenzweig, *Nature* 434 (2005) 177;
 (e) E.W.C.E. Arends, P. Gamez, R.A. Sheldon, in: R. Eldijk, J. Reedijk (Eds.), *Advances in Inorganic Chemistry*, vol. 58, Elsevier, Amsterdam, 2006, p. 235;
 (f) R.G. Stenkamp, *Chem. Rev.* 94 (1994) 715.
- D.H.R. Barton, A.E. Martell, D.T. Sawyer, *The Activation of Dioxygen and Homogeneous Catalytic Oxidation*, Plenum, New York, 1993.
- (a) For recent reviews on the use of molecular oxygen as oxidant see: Z. Shi, C. Zhang, C. Tang, N. Jiao, *Chem. Soc. Rev.* 41 (2012) 3381;
 (b) J. Piera, J.-E. Backvall, *Angew. Chem. Int. Ed.* 47 (2008) 3506;
 (c) X. Shan, L. Que Jr., *J. Inorg. Biochem.* 100 (2006) 421;
 (d) T. Punniyamurthy, S. Velusamy, J. Iqbal, *Chem. Rev.* 105 (2005) 2329;
 (e) R.A. Sheldon, I.W.C.E. Arends, G.-J.T. Brink, A. Dijkman, *Acc. Chem. Res.* 35 (2002) 774.
- B. Meunier (Ed.), *Biomimetic Oxidations Catalyzed by Transition Metal Complexes*, Imperial College Press, London, 2000.
- M.J. Goldcamp, J.A. Krause, S.E. Robinson, M.J. Baldwin, *Inorg. Chem.* 41 (2002) 2307.
- (a) S.E. Edison, R.P. Hotz, M.J. Baldwin, *Chem. Comm.* (2004) 1212;
 (b) M.J. Baldwin, J.A. Krause, M.J. Goldcamp, M. Haven, S.E. Edison, L.N. Squires, *Bioinspired Aerobic Substrate Oxidation*, ACS Symposium Series, vol. 1012, Chapter 9, 2009, p. 133;
 (c) S.E. Edison, S.D. Conklin, N. Kaval, L.E. Cheruzel, J.A. Krause, C.J. Seliskar, W.R. Heineman, R.M. Buchanan, M.J. Baldwin, *Inorg. Chim. Acta* 361 (2008) 947.
- (a) A.N. Singh, A. Chakravorty, *Inorg. Chem.* 19 (1980) 969. and references cited therein;
 (b) S.J. Kim, T. Takizawa, *Die Makromol. Chem.* 175 (1974) 125.
- (a) A.N. Semakin, A.Yu. Sukhorukov, A.V. Lesiv, Yu.A. Khomutova, S.L. Ioffe, K.A. Lyssenko, *Synthesis* (2007) 2862;
 (b) A.N. Semakin, A.Yu. Sukhorukov, Yu.A. Khomutova, S.L. Ioffe, *Synthesis* (2011) 1403.
- A.D. Dilman, A.A. Tishkov, I.M. Lyapkalo, S.L. Ioffe, Yu.A. Strelenko, V.A. Tartakovskiy, *Synthesis* (1998) 181.

- [11] M.J. Goldcamp, S.E. Edison, L.N. Squires, D.T. Rosa, N.K. Vowels, N.L. Coker, J.A. Krause Bauer, M.J. Baldwin, *Inorg. Chem.* 42 (2003) 717.
- [12] (a) A.Yu. Sukhorukov, I.V. Bliznets, A.V. Lesiv, Yu.A. Khomutova, S.L. Ioffe, *Synthesis* (2005) 1077;
(b) A.Yu. Sukhorukov, A.N. Semakin, A.V. Lesiv, Yu.A. Khomutova, S.L. Ioffe, *Zh. Org. Khim.* 43 (2007) 1118. *Russ. J. Org. Chem. (Engl. Transl.)* 43 (2007) 1106.
- [13] (a) R. Jones, M.J. Baldwin, *J. Phys. Chem. A* 108 (2004) 3537;
(b) R. Jones, M.J. Goldcamp, J.A. Krause, M.J. Baldwin, *Polyhedron* 25 (2006) 3145.
- [14] (a) Programs, SAINT and SADABS, 1999.;
(b) G.M. Sheldrick, *Acta Crystallogr., Sect. A* 64 (2008) 112;
(c) . CSD, release 2013F.H. Allen, *Acta Crystallogr., Sect. B* 58 (2002) 380.
- [15] (a) B. Hsu, E.O. Schlemper, C.K. Fair, *Acta Crystallogr., Sect. B* 36 (1980) 1387;
(b) E.O. Schlemper, V.C. Hamilton, S.J. La Placa, *J. Chem. Phys.* 54 (1971) 3990.
- [16] E. Dieters, M.J. Goldcamp, J.A. Krause Bauer, M.J. Baldwin, *Inorg. Chem.* 44 (2005) 5222.
- [17] D. Natale, J.C. Mareque-Rivas, *Chem. Commun.* (2008) 425.
- [18] H.-B. Ji, T.-T. Wang, M.-Y. Zhang, Q.-L. Chen, X.-N. Gao, *React. Kinet. Catal. Lett.* 90 (2007) 251.